

Transport properties of nonlinear double-barrier structures

Enrique Diez and Angel Sánchez

Escuela Politécnica Superior, Universidad Carlos III de Madrid, C./ Butarque 15, E-28911 Leganés, Madrid, Spain

Francisco Domínguez-Adame

Departamento de Física de Materiales, Facultad de Físicas, Universidad Complutense, E-28040 Madrid, Spain

We introduce a solvable model of a nonlinear double-barrier structure, described by a generalized effective-mass equation with a nonlinear coupling term. This model is interesting in its own right for possible new applications, as well as to help understand the combined effect of spatial correlations and nonlinearity on disordered systems. Although we specifically discuss the application of the model to electron transport in semiconductor devices, our results apply to other contexts, such as nonlinear optical phenomena. Our model consists of finite width barriers and nonlinearities are dealt with separately in the barriers and in the well, both with and without applied electric fields. We study a wide range of nonlinearity coupling values. When the nonlinear term is only present in the barriers, a sideband is observed in addition to the main resonance and, as a consequence, the current-voltage characteristics present two peaks at different voltages. In this case, the phenomenology remains basically the same through all the considered variation of the parameters. When the well is the component exhibiting nonlinearity, the results depend strongly on the nonlinear coefficient. For small values, the current-voltage characteristics exhibit lower and upper voltage cutoffs. This phenomenon is not present at higher nonlinearities, and eventually linear-like behavior is recovered. We complete this exhaustive study with an analysis of the effects of having simultaneously both kinds of nonlinear couplings. We conclude the paper with a summary of our results, their technological implications, and a prospective discussion of the consequences of our work for more complex systems.

I. INTRODUCTION

This decade is witnessing a rapid increase of the amount of effort devoted to the study of one-dimensional (1D) systems, for reasons both theoretical and technological. In particular, emphasis is being put on localization and delocalization in non-spatially-periodic (quasiperiodic or disordered) problems, which are relevant in very many contexts. From the fundamental viewpoint, research is being conducted in two different main directions. On the one hand, the generality of localization phenomena in 1D systems has recently been questioned in a number of papers,^{1,2} which have shown that the introduction of short-range correlation in the distribution of inhomogeneities leads to the formation of bands of extended states. This unexpected phenomenon can be understood in terms of the structure of the transmission coefficient for different segments of the considered system.³ On the other hand, nonlinear effects have also been proposed to counteract the localizing influence of disorder on waves of any nature (see, e.g., the reviews in Ref. 4 and references therein). Unfortunately, the results of the interplay between disorder and nonlinearity depend to a certain extent on the specific model considered and a general theory of this problem is still lacking (see, for instance, Refs. 4 and 5 and references therein).

Following along the above line of research, in this pa-

per we concern ourselves with the study of a nonlinear double-barrier resonant structure. Recently, several authors have reported research on related devices: For instance, a mean field analysis of multiple resonant tunneling exhibiting chaotic behavior has been carried out by Presilla, Jona-Lasinio, and Capasso;⁶ in a different context, directional couplers including nonlinear elements have been investigated as optical switches.⁷ The model we propose shares some of the characteristics of these: Specifically, it is described by a Schrödinger equation where an effective nonlinearity is included and, being formally close to effective nonlinear Schrödinger equations arising in other problems, it is also very general. However, we are going to be mostly interested in its application to resonant tunneling (RT) through semiconductor heterostructures. This phenomenon, which takes place in linear double-barrier structures (DBS), make these systems very promising candidates for a new generation of ultra-high speed electronic devices: For instance, a GaAs-Ga_{1-x}Al_xAs DBS operating at THz frequencies has already been reported in the literature.⁸

The basic reason for RT to arise in DBS is a quantum phenomenon whose fundamental characteristics are by now well understood: There exists a dramatic increase of the electron transmitivity whenever the energy of the incident electron is close to one of the unoccupied quasi-bound-states inside the well.⁹ In practice, a

bias voltage is applied to shift the energy of this quasi-bound-state of nonzero width so that its center matches the Fermi level. Consequently, the $j - V$ characteristics present negative differential resistance (NDR). In actual samples, however, the situation is much more complex than this simple picture. This is so even in good-quality heterostructures, when scattering by dislocations or surface roughness is negligible. In particular, *inelastic* scattering is always present in real devices. Examples of inelastic scattering events are electron-lattice and electron-electron interactions, in which the energy of the tunneling electron changes and the phase memory is lost. Strong local coupling between electronic and vibrational degrees of freedom (i.e., when electrons propagate in a deformable charged medium) leads to a self-induced attractive force which we will account for by means of an effective nonlinearity as discussed below. Moreover, Hartree-type repulsive interactions between electrons can be viewed as a self-induced repulsive force within an effective medium framework. There are currently available very many materials with different optical or electrical nonlinear properties, and then it may be possible to purposely build nonlinear DBS structures like those we work with. In view of this, the question arises as to whether such nonlinear devices will have characteristics of interest for applications. In any case, it seems that the (intentional or not) introduction of nonlinearity is going to have non-trivial consequences on the linear phenomenon of RT, and our purpose here is to study how RT is so modified as well as to analyze its measurable consequences.

Aside from the above technological and experimental motivations, the research we summarize in this paper has further goals. We have recently studied how short-range spatial correlations affect electron localization, both theoretically,^{2,3} (even including possible three-dimensional effects, see Ref. 10) and from the viewpoint of real nanoelectronic devices.¹¹ In this paper, what we also intend to address is the question of how nonlinearity modifies our conclusions about linear correlated disordered systems. We have already posed this problem in a preliminary work,¹² where we considered concentrated nonlinearities using point-like barriers described by δ -function potentials. Nevertheless, such a situation is rather academic and, in addition, we have shown, for the case of linear correlated systems, that the results change dramatically when the width of the barriers is not neglected.¹¹ Therefore, similar variations may (and should be expected to) occur in the nonlinear problem when the barrier widths are taken into account, and this has to be done if any prediction is to be relevant for actual experiments or devices.

The paper is organized as follows. In Sec. II we present our model, obtained by including a nonlinear coupling in a generalized effective-mass equation. We particularize it for a DBS but we insist that the model is quite general and applicable in different physical contexts. We discuss in detail the physics underlying our choice for the coupling. We sketch the exact solution of the model, as well

as the way to obtain the transmission coefficient as a function of the nonlinear couplings and the applied voltage V . For completeness, we include an appendix containing a brief discussion of the range of applicability of the equation and its connection with physical interpretations. Afterwards, Sec. III contains the main results and discussions of our analysis concerning the application to semiconductor heterostructures, namely electron transmission and $j - V$ characteristics. We also analyze how the results are changed by the simultaneous presence of both types of nonlinearity. Finally, Sec. IV concludes the paper with a brief survey of the results and some prospects on the application of the ideas we have discussed.

II. MODEL

A. Physical grounds and definitions

As we announced in the introduction, to describe our model we have chosen to apply it to a specific system: A semiconductor DBS under an applied electric field. In the following, we will be using parameters corresponding to GaAs-Ga_{1-x}Al_xAs as typical values for the linear DBS, whereas the nonlinear terms will be taken at most as a few percents of the built-in potential. Larger nonlinearities are not considered because they may invalidate from the beginning the approximations involved in our theoretical calculation and, besides, they may make impossible to find any material with the desired properties, at least in the context of electron transport. Our choices are thus as follows. The thickness of the whole structure is L and the thickness of the well is d . The barriers are assumed to be of the same thickness (symmetric case) but as will be evident below this is not a restriction of our approach. The structure is embedded in a highly doped material acting as contact, so that the electric field is applied only in the DBS. We focus on electron states close to the bandgap and thus we can neglect nonparabolicity effects hereafter. Then the one-band effective-mass framework is completely justified to get accurate results. For the sake of simplicity, we will further assume that the electron effective-mass m^* and the dielectric constant are the same in both materials. This hypothesis is related to the fact that we are not interested in high quantitative accuracy, although we note that the spatial dependence of these parameters can be taken into account if necessary.

Within this approach, the electron wave function is written as a product of a band-edge orbital with a slowly varying envelope-function. Therefore the envelope-function $\psi(z)$ satisfies a generalized effective-mass equation (we use units such that energies are measured in effective Rydberg, Ry*, and lengths in effective Bohr radius, a*, being 1 Ry* = 5.5 meV and 1 a* = 100 Å in GaAs) given by

$$-\psi_{zz}(z) + [V(z) - eFz] \psi(z) = E \psi(z), \quad (1)$$

where $V(z)$ is the potential term which we discuss below and F is the electric field applied along the growth direction. We note, in connection with the generality of our model, that equations similar to Eq. (1) are used to describe light or other electromagnetic wave propagation in dielectric superlattices, in an approximation where only the scalar nature of the waves is taken into account.⁷ We now specify our model by choosing what is the potential term $V(z)$. In order to do that, let us first consider the physics we are trying to represent with this term. The DBS can be regarded as an effective medium which reacts to the presence of the tunneling electron, leading to a feedback mechanism by which inelastic scattering processes change the RT characteristics of the device. It thus follows that $V(z)$ must contain nonlinear terms if it is to summarize the medium reaction which comes from the electron-electron and electron-lattice interactions. The simplest candidate to contain this feedback process is the charge density of the electron, which is proportional to $|\psi(z)|^2$. In our model, we neglect higher order contributions and postulate that the potential in Eq. (1) has the form

$$V(z) = V_0 \left\{ [1 + \tilde{\alpha}|\psi(z)|^2] \chi_b(z) + \tilde{\beta}|\psi(z)|^2 \chi_w(z) \right\}, \quad (2)$$

where V_0 is the conduction band-offset at the interfaces, and $\chi_b(z)$ and $\chi_w(z)$ are respectively the characteristic functions of the barriers and the well,

$$\chi_b(z) = \begin{cases} 1, & \text{if } 0 < z < (L-d)/2, \\ 1, & \text{if } (L+d)/2 < z < L, \\ 0, & \text{otherwise,} \end{cases} \quad (3a)$$

$$\chi_w(z) = \begin{cases} 1, & \text{if } (L-d)/2 < z < (L+d)/2, \\ 0, & \text{otherwise.} \end{cases} \quad (3b)$$

and all the nonlinear physics is contained in the coefficients $\tilde{\alpha}$ and $\tilde{\beta}$ which we discuss below.

There are two factors that configure the medium response to the tunneling electron. First, it goes without saying that there are repulsive electron-electron Coulomb interactions, which should enter the effective potential with a positive term proportional to the charge, i.e., the energy is increased by local charge accumulations, leading to a positive sign for $\tilde{\alpha}$ and $\tilde{\beta}$. On the other hand, in polar semiconductors, the electron polarizes the surrounding medium creating a local, positive charge density. Hence the electron reacts to this polarization and experiences an attractive potential, which implies $\tilde{\alpha}$ and $\tilde{\beta}$ negative. This happens, for instance, in the polaron problem in the weak coupling limit, which becomes valid in most semiconductors, and where it can be seen that the lowest band energy state decreases.¹³ It is then clear that in principle any sign would be equally possible for the coefficients if $\tilde{\alpha}$ and $\tilde{\beta}$ are to represent the combined

action of the polarization of the lattice along with repulsive electron-electron interactions. Intuitively, however, it is most realistic to think that $\tilde{\alpha}$ will be negative, because a positive nonlinear interaction would arise from negative charge accumulation in the barriers, which is not likely to occur. However, as far as the well is concerned, this is not so, because charge does tend to accumulate between the two barriers. This is the case considered, for instance, in the works of Presilla *et al.*⁶ where they introduce a term in the Schrödinger equation proportional to the total charge in the well (the integral of the square of the wavefunction). Notice as we are going to apply a field to the DBS, high charge values will not build up between the two barriers, at least for low doping levels. Therefore, we will assume that lattice polarization effects are stronger than electron-electron interactions inside the well, thus leading to a negative $\tilde{\beta}$. On the other hand, we discuss below mathematical reasons imposing that $\tilde{\alpha}$ and $\tilde{\beta}$ have to be negative as expected, allowing for it to be positive only if they are small. This will be shown there to stem from the fact that we are studying a boundary value problem for an ordinary differential equation, and therefore the case of positive couplings is restricted to a fully dynamical study, which will be the subject of further work.¹⁴

B. Analytical results

We now work starting from Eq. (1) with the definition in Eq. (2) to cast our equations in a more tractable form. For simplicity, and because we are interested in intrinsic DBS features, we consider that the contacts in which the structure is embedded behave linearly. Therefore, the solution of Eq. (1) is a linear combination of traveling waves. As usual in scattering problems, we assume an electron incident from the left and define the reflection, r , and transmission, t , amplitudes by the relationships

$$\psi(z) = \begin{cases} A (e^{ik_0 z} + r e^{-ik_0 z}) & z < 0, \\ A t e^{ik_L z} & z > L, \end{cases} \quad (4)$$

where $k_0^2 = E$, $k_L^2 = E + eFL$, and A is the incident wave amplitude. Now we define $\psi(z) = A\phi(z)$, $\alpha = \tilde{\alpha}|A|^2$, and $\beta = \tilde{\beta}|A|^2$. Notice that α and β are dimensionless parameters and that they depend on the amplitude of the incoming wave, which will be relevant later. Using Eq. (1) we get

$$-\phi_{zz}(z) + [V(z) - eFz - E] \phi(z) = 0. \quad (5)$$

To solve the scattering problem in the DBS we develop a similar approach to that given in Ref. 15. Since $\phi(z)$ is a complex function, we write $\phi(z) = q(z) \exp[i\gamma(z)]$, where $q(z)$ and $\gamma(z)$ are real functions. Inserting this factorization in Eq. (5) we have $\gamma_z(z) = q^{-2}(z)$ and

$$\begin{aligned} -q_{zz}(z) + \frac{1}{q^3(z)} + [V_0 \chi_b(z) - eFz - E] q(z) + \\ + V_0 [\alpha \chi_b(z) + \beta \chi_w(z)] q^3(z) = 0. \end{aligned} \quad (6)$$

This nonlinear differential equation must be supplemented by appropriate boundary conditions. However, using Eq. (4) this problem can be converted into a initial conditions equation. In fact, it is straightforward to prove that

$$q(L) = k_L^{-1/2}, \quad q_z(L) = 0, \quad (7)$$

and that the transmission coefficient is given by

$$\tau = \frac{4k_0 q^2(0)}{1 + 2k_0 q^2(0) + k_0^2 q^4(0) + q^2(0) q_z^2(0)}. \quad (8)$$

Hence, we can integrate numerically (6) with initial conditions (7) backwards, from $z = L$ up to $z = 0$, to obtain $q(0)$ and $q_z(0)$, thus computing the transmission coefficient for given nonlinear couplings α and β , incoming energy E and applied voltage $V = FL$.

Once the transmission coefficient has been computed, and recalling that contacts are linear media, the tunneling current density at a given temperature T for the DBS can be calculated within the stationary-state model from

$$j(V) = \frac{m^* e k_B T}{2\pi^2 \hbar^3} \int_0^\infty \tau(E, V) N(E, V) dE, \quad (9a)$$

where $N(E, V)$ accounts for the occupation of states to both sides of the device, according to the Fermi distribution function, and it is given by

$$N(E, V) = \ln \left(\frac{1 + \exp[(E_F - E)/k_B T]}{1 + \exp[(E_F - E - eV)/k_B T]} \right), \quad (9b)$$

where k_B is the Boltzmann constant.

III. RESULTS AND DISCUSSIONS

In our calculations we have considered a GaAs-Ga_{0.65}Al_{0.35}As double-barrier structure with $L = 3d = 150$ Å. The conduction-band offset is $V_0 = 250$ meV. In the absence of applied electric field and nonlinearities, there exist a single, very narrow resonance with $\tau \sim 1$ below the top of the barrier, with an energy of 80.7 meV, and hence the well supports a single quasi-bound state. When voltage is applied, the energy of the quasi-bound state level is lowered and a strong enhancement of the current arises whenever the Fermi level matches this resonance, thus leading to the well-known RT phenomenon. As we will see, it is enough to have a small amount of nonlinearity to have this picture changed dramatically. In this respect, before entering our report, we want to stress that the coefficients α and β that we have defined depend not only on the intrinsic characteristics of the material but also on the energy of the incoming electrons, as they both include the factor $|A|^2$. Therefore, it makes sense to study different values for the two coefficients, because even for the same device transport properties can be very different for different incoming electrons.

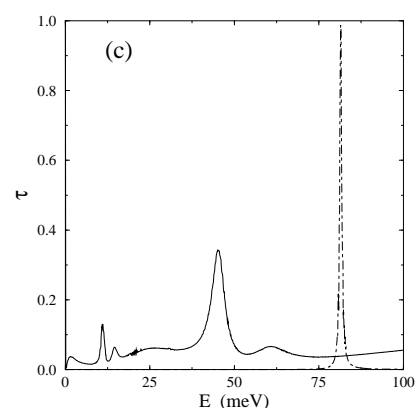
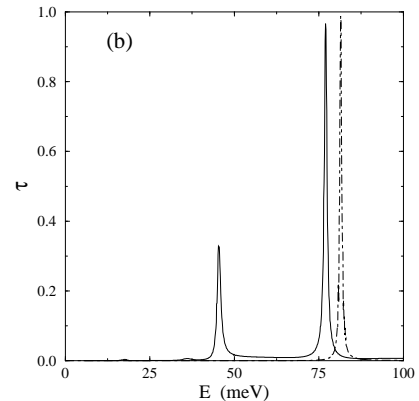
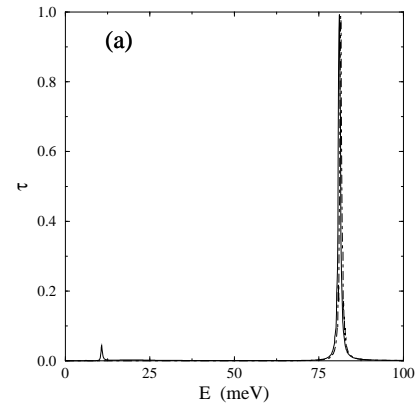


FIG. 1. Transmission coefficient τ as a function of the electron energy at zero bias for (a) $\alpha = -0.001$, (b) -0.01 , and (c) -0.1 . For comparison, dashed line indicates the result for $\alpha = 0$.

A. Nonlinear barriers

We will begin by discussing the effects of having nonlinearity in the barriers only ($\beta = 0$), and our starting point will be to report on zero field transmission properties. We will consider three values for α , $\alpha = -0.001, -0.01, -0.1$, as representatives of very different orders of magnitude. Hereafter, for brevity of language we will call *large* values of the nonlinearity to those large in absolute value. For the purposes of the present paper we will regard values larger than those quoted above as not physically realizable, although in principle materials with such exotic properties might be found; smaller values behave mostly like the linear system. Figure 1 shows the transmission coefficient as a function of the incoming energy for these three different values of the coefficient α , when the DBS is placed under zero bias. It is seen that for the two lower values there exist two peaks, but the smallest one is only well differentiated for $\alpha = -0.01$. The main peak is centered at ~ 75 meV (close to the linear case peak) and the sideband is centered at ~ 40 meV for $\alpha = -0.01$. Compared to the purely linear case, the main peak not only shifts to lower energies but also broadens, in a similar fashion to what happens in RT when inelastic effects arise, and this shifting and broadening is larger when α increases. Upon further increasing α , the sideband moves below zero, whereas the main peak reduces appreciably, as shown in Fig. 1(c). We thus see that the effect of strong nonlinearity becomes simply to move down and broaden the main peak, and therefore the existence of two peaks belongs only to a limited range of α .

In order to gain insight into this phenomenon, we can rewrite Eq. (5) as follows

$$-\phi_{zz}(z) + V_{eff}(z, E) \phi(z) = E \phi(z), \quad (10a)$$

where we have defined an effective potential as follows

$$V_{eff}(z, E) = V_0 \chi_b(z) [1 + \alpha q^2(z)] - eFz. \quad (10b)$$

Thus (10) is a Schrödinger-like equation for an effective potential due to nonlinearity plus the linear potential and the built-in potential of the DBS. This effective potential depends not only on z but also on the incoming energy E through the function $q(z)$. Let us analyze its meaning in the zero field situation. Since the envelope function changes under RT conditions, and also does $q(z)$, it should be expected that $V_{eff}(z, E)$ undergoes severe variations whenever E is close to one of the RT peaks. This is indeed the case, as shown in Fig. 2, where $V_{eff}(z, E)$ is displayed at zero bias for $\alpha = -0.01$ as a representative example of all the studied values. Notice that nonlinear effects have negligible effects on the shape of the effective potential in the right barrier, besides a slight band bending at the interface $z = (L + d)/2$ at low energies. However, the potential in the left barrier region differs significantly from the original square-barrier shape. Out of energy resonances, the effective barrier height at $z = 0$

is lower than V_0 , whereas at resonances it takes the value $\sim V_0$. This is clearly related to the ability of the electrons to go through the structure for the resonant energies and their subsequent low probability of remaining inside the barrier. Hence the effective potential presents two local maxima in the plane $z = 0$ as a function of the incoming energy E , matching the values of the main resonance and the sideband above discussed. From Fig. 2 it is clear that at the energy of the main resonance the effective potential is quite similar to the built-in DBS potential, just producing a small shift of the quasi-bound-state in comparison to the linear RT process. Concerning the sideband, the effective potential presents a deep minimum at the interface $z = (L - d)/2$, which originates another quasi-bound-state, thus explaining the origin of this lower RT peak. Indeed, the fact that this added well is responsible for the peak is confirmed by observations of the effective potential when fields are applied, as discussed below. Another reason supporting this hypothesis is that for the smallest α the sideband is located at a lower energy, which makes sense since in that case the depth of the extra well is smaller. We thus provide a complete coherent picture of the zero field tunneling phenomenology.

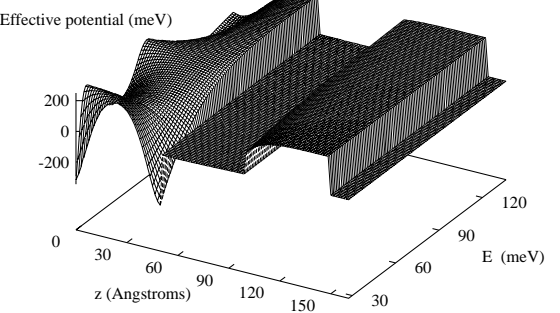


FIG. 2. Effective potential V_{eff} as a function of z and the incoming electron energy E at zero bias, for $\alpha = -0.01$.

We now consider the effect of a bias imposed on the DBS and show an example of the general behavior for all the considered values of α in Fig. 3. The transmission peaks are shifted to smaller values of energy, leading first, in the cases when there is a sideband, to the suppression of this subsidiary peak, as can be seen by comparing Figs. 3 (a) and (b). In this respect, we have to say that such shift to lower energies is similar to that found in linear (coherent) RT. Now we can conclude the interpretation of our findings in terms of the effective potential as announced. By reasoning in the same way as above but taking the field into account, we have concluded that the fact that the resonance responsible for the peak shifts towards $E = 0$ is due to the influence of the applied field, which increases the depth of the secondary well; the second resonance goes subsequently below zero and ceases

to be seen in the transmission coefficient. Afterwards, for higher fields, even the main peak is suppressed by the same mechanism, although if even higher fields are applied, new levels are bound by such a deeper well. We do not go further into the details of those as we are interested in the small fields suitable for our approximations and for application to actual devices.

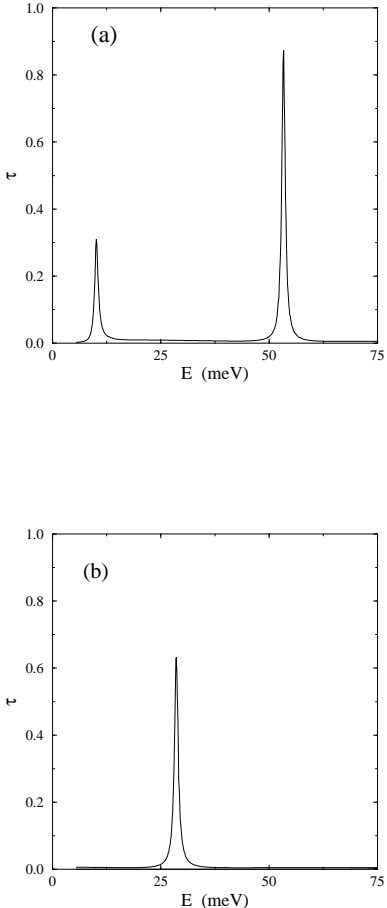


FIG. 3. Transmission coefficient τ as a function of the electron energy for $\alpha = -0.01$ with (a) $V = 0.05$ volts and (b) 0.10 volts.

We are now in a position where we are able to comment on the $j-V$ characteristics, computed from (9). We have set two different temperatures (77 K and room temperature) and compared these curves with those obtained in linear RT. The Fermi energy was $E_F = 27.5$ meV. We discuss the lower α cases first, shown in Fig. 4. We have not plotted the curve for $\alpha = -0.001$ as it turns out to be almost indistinguishable from the linear one, which always shows a single NDR peak. When $\alpha = -0.01$, at $T = 77$ K nonlinearity causes the occurrence of a second peak at a lower voltage, clearly related to the sideband

in the transmission coefficient.

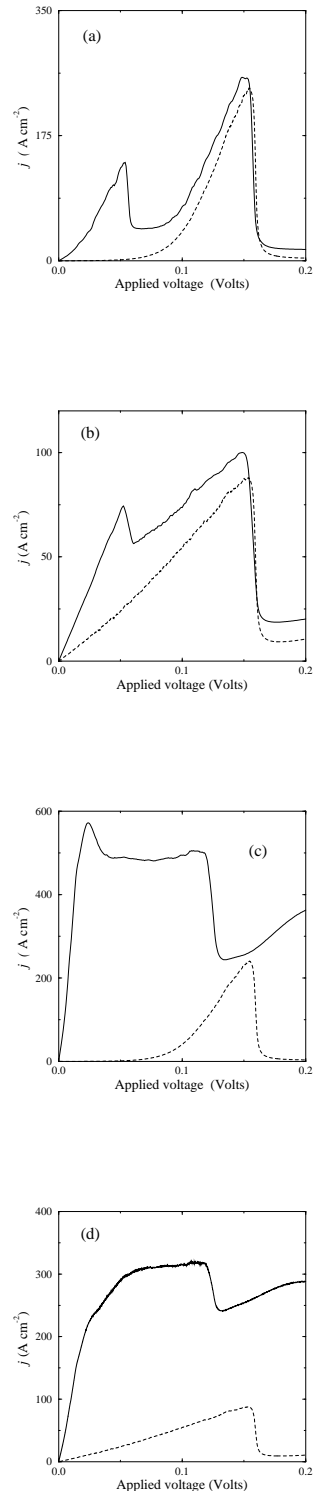


FIG. 4. Computed $j-V$ characteristics for $E_F = 27.5$ meV, $\alpha = -0.01$ at (a) $T = 77$ K and (b) room temperature, and $\alpha = -0.1$ at (c) $T = 77$ K and (d) room temperature. For comparison, dashed line indicates the result for $\alpha = 0$.

On increasing temperature up to room values, both peaks merge into a single one because of the broadening of the Fermi-Dirac distribution function. It is important to notice that the $j-V$ characteristics collect all the main features found in the transmission coefficient, namely a downwards shifting of the main RT peak, its corresponding broadening due to inelastic effects and the appearance of the sideband, as shown in Fig. 4(a) and (b) as a smaller NDR signature at $V = 0.05$ volts. As for the results for $\alpha = -0.1$, they exhibit related features although somewhat less prominent and shifted towards lower voltages [see Fig 4(c) and (d)]. The disappearance of the sideband for this nonlinearity value leads to a structure of the $j-V$ curve different than the previous one, which consists of a plateau starting at low voltage values. This is connected to the nonzero value of the transmission coefficient [see Fig. 1(c)] for all energies, which allows for transmission even in non-RT conditions. The end of the plateau is an NDR interval which is associated to the broad peak originated by the linear resonance. In addition, the current is twice as large as for the previous case. Following the plateau, the current drops down but it does not reach zero values, rather it keeps at a value about half that of the plateau. This is even more clear from the room temperature plot, which shows practically no features, i.e., loosely speaking, the current tends to be constant. The current values the DBS supports are clearly larger than in the linear and weakly nonlinear cases.

B. Nonlinear well

Let us now turn our attention to the case when $\alpha = 0$, i.e., only the well in the DBS is nonlinear, which turns to be out very different from the previously discussed nonlinear barrier DBS. Results for the transmission coefficient at zero field are shown in Fig. 5. From those plots, it can be seen that in general the effect of β is more dramatic than that of α , and that the case when $\beta = -0.001$ has not much to do with the other two values. For the smallest nonlinearity, we see two peaks (as in the intermediate α case), but the main one has departed largely from the linear resonance. This is related to the fact that β is negative, and therefore, accumulation of charge inside the well makes it deeper, thus moving the resonant quasilevel to lower energies. Increasing β will eventually locate the resonance below the zero energy and thus the appearance of the plots for $\beta = -0.01$ and $\beta = -0.1$. The less pronounced peaks appearing (meaning, for $\beta = -0.001$, the one playing the role of the sideband) have to do with the deformation of the bottom of the well by the spatial distribution of the charge. This can again be understood from the same effective potential ideas discussed in the previous subsection: By inspecting Fig. 6, where the effective potential is shown for the intermediate and large β values, it is clear that tunneling of electrons inside the well changes its structure dramatically, at first even splitting

it into two [Fig. 6(a)] or several [Fig. 6(b)] wells.

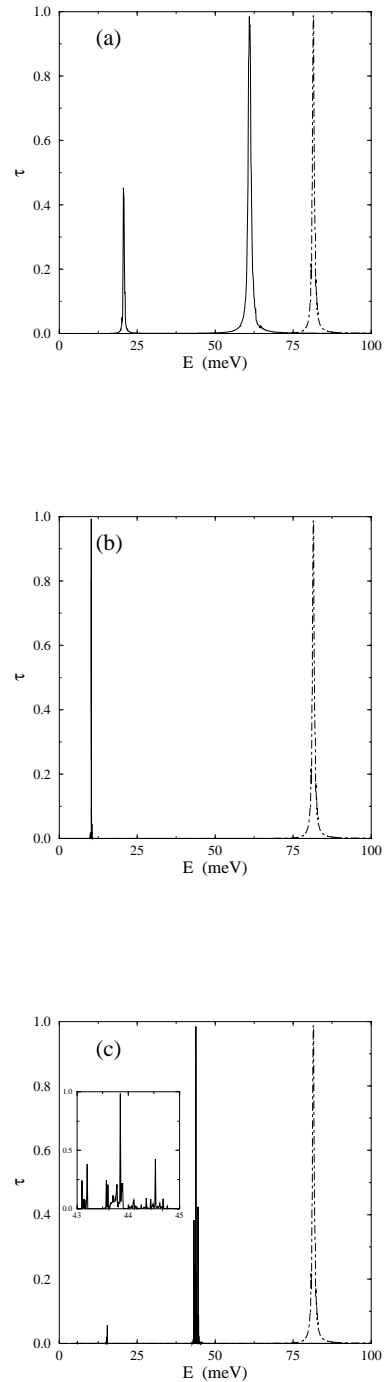


FIG. 5. Transmission coefficient τ as a function of the electron energy for (a) $\beta = -0.001$, (b) -0.01 , and (c) -0.1 . The inset shows an enlarged view of the transmission coefficient close to 45 meV. For comparison, dashed line indicates the result for $\beta = 0$.

The main point in that picture is that for the largest nonlinearity, the depth of the well is much larger than in the linear case, and therefore the main resonance is now located at negative energies, this being the reason for the disappearance of the main peak in the transmission coefficient. Besides, the complicated structure of the bottom of the well in [Fig. 6(b)] helps understand why the peak appearing in the transmission coefficient exhibits structure; coupling between the subwells induces splitting of the quasi-level into several subresonances responsible for this finest features of the transmission coefficient [see the inset of Fig. 5(c)].

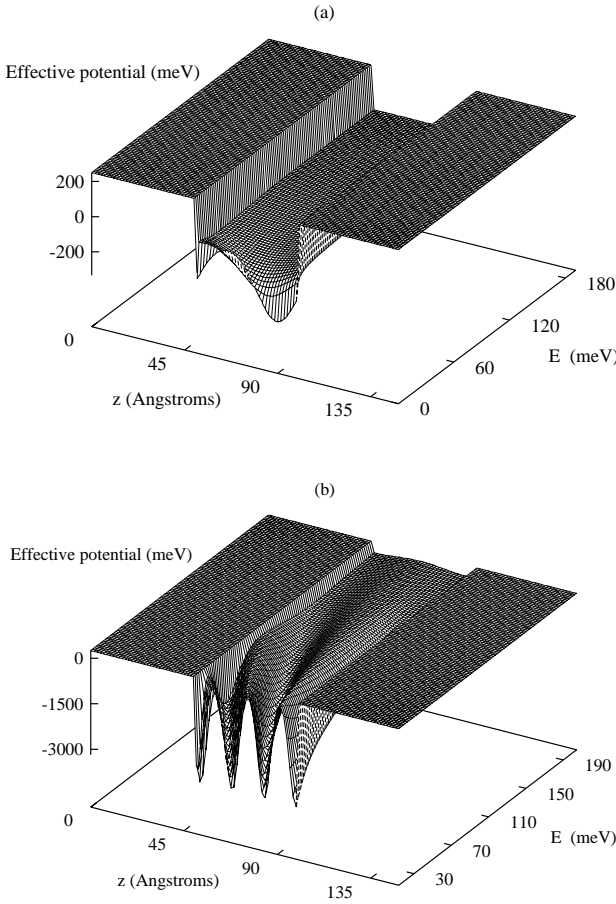
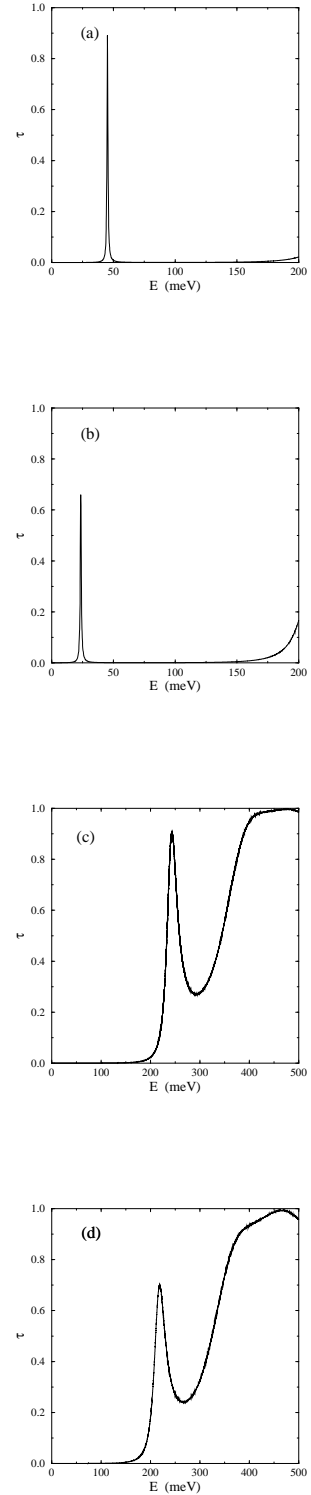


FIG. 6. Effective potential V_{eff} as a function of z and the incoming electron energy E at zero bias for (a) $\beta = -0.001$ and (b) -0.1 .

When bias is applied to the slightly nonlinear well ($\beta = -0.001$), the structure of the transmission coefficient changes very smoothly, see Fig. 7, much as in the nonlinear barrier case. Due to the increased presence of electrons in the well induced by the field, the resonant level goes down and so does the transmission coefficient peak. Remarkably, the intermediate nonlinearity ($\beta = -0.01$) is such that there is no peak at all in the transmission coefficient, although for the largest field

value it is seen that one is entering from above. This will have consequences on the $j - V$ curves which will be discussed below.



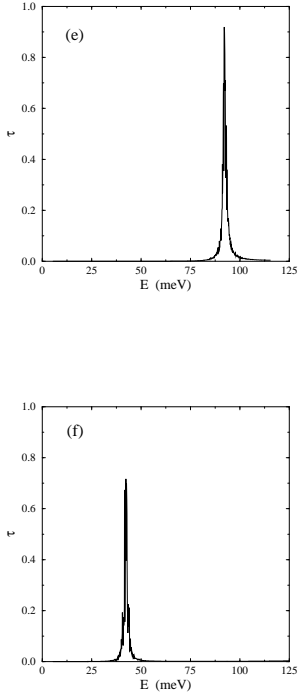


FIG. 7. Transmission coefficient τ as a function of the electron energy for $\beta = -0.001$ with (a) $V = 0.05$ volts and (b) 0.10 volts; $\beta = -0.01$ with (c) $V = 0.05$ volts and (d) 0.10 volts; $\beta = -0.1$ with (e) $V = 0.05$ volts and (f) 0.10 volts.

For $\beta = -0.1$, the field increases the inner structure of the peaks but for the rest they behave as in the other cases, moving downwards when increasing the field. In view of the effective potential structure, this probably has to do with the fact that when the field is applied the tilting of the well induces the appearance of a positive energy quasi-level, whose energy decreases with increasing field and, subsequently, with increasing well depth. Larger fields destroy this structure, suppressing this quasi-level. The different behavior for the values of β considered reflects in the $j - V$ characteristics as well. We only show the results at $T = 77$ K because those at room temperature are essentially the same, scaled down by a factor one half. In Fig. 8(a) it can be seen that the case $\beta = -0.001$ is practically identical to the $\alpha = -0.01$ case, which is reasonable in view that they both have the same transmission coefficient structure, albeit for different reasons. The main differences between those two devices are that for this nonlinear well one we are discussing, the first peak appears for much smaller values of the voltage, and that it shows a lot of structure coming from the inner wells induced in the quantum well. Upon increasing the value of β , it is found that, interestingly, intermediate β values suppress completely the current [Fig. 8(b)], a phenomenon that is evidently connected with the absence of resonances for that β value already reported. However, the case of large β shows a very unexpected feature: A

series of noisy peaks appears when the nonlinear DBS starts conducting, which we tentatively associate to the structure of the well in this highly nonlinear case. For the rest, the DBS behaves qualitatively as in the linear case, as seen in Fig. 8(c).

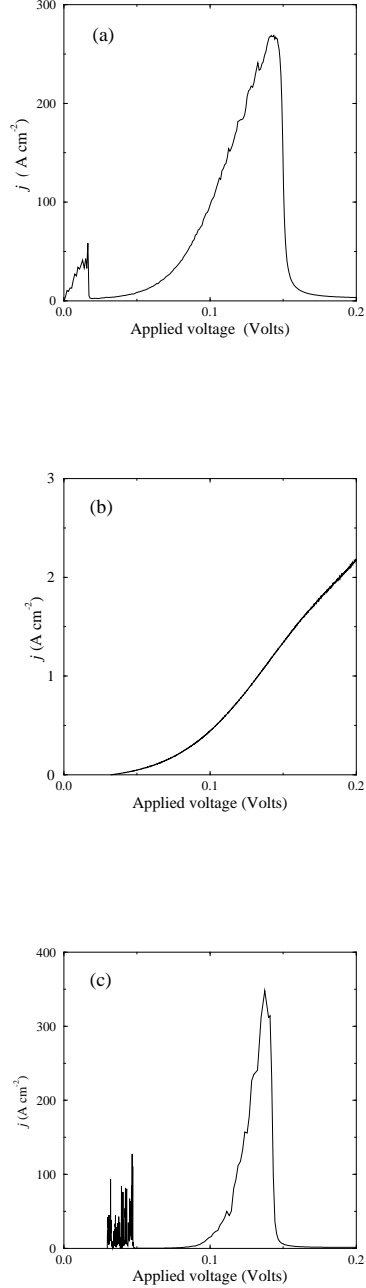


FIG. 8. Computed $j - V$ characteristics for $E_F = 27.5$ meV, $T = 77$ K and (a) $\beta = -0.001$, (b) -0.01 , and (c) -0.1 . Note that the scale in (b) is much smaller than in the other two ones. Results at room temperature at the same although scaled by one half.

C. Fully nonlinear DBS

When both constituents of the DBS, i.e., the barriers and the well, are nonlinear, the number of possibilities is of course considerably augmented. It is not our aim to study thoroughly all possible combinations in this section, but rather, to present a brief idea of what can be said about this more complex devices.

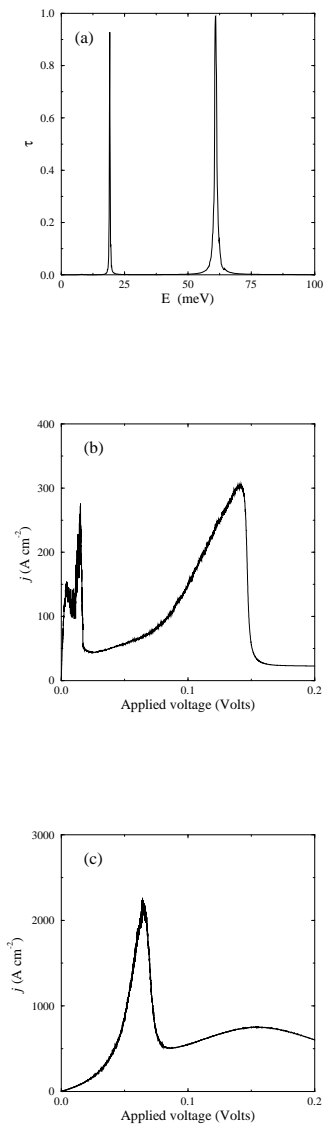


FIG. 9. (a) Transmission coefficient τ as a function of the electron energy for $\alpha = \beta = -0.001$. (b) $j - V$ curve for $\alpha = 10\beta = -0.01$ and $T = 77$ K. (c) $j - V$ curve for $\alpha = \beta = -0.1$ and $T = 77$ K.

After an exploration of the main possibilities, we concluded that for small and intermediate α (barrier nonlinearity), it is the nonlinearity of the well, β , the one

that governs the behavior of the system. Thus, for $\beta = -0.001$, the structure of the transmission coefficient shows two peaks until $\alpha = -0.1$ which leads to a smoothing out of the peaks by almost suppression of the barriers. Indeed, the two peak structure is even clearer when $\beta = \alpha = -0.001$ than in the other cases discussed so far [see Fig. 9(a)], and as consequence so is the two NDR peak feature of the $j - V$ curve. The only difference between $\alpha = -0.001$ and $\alpha = -0.01$ is that this last choice always gives rise to a somewhat more complicated curve [see an example in Fig. 9(b)]. On the other hand, when α is large, then it is this factor the one responsible for the behavior of the DBS, except when β is also large (thus compensating the decreasing of the barriers). In that case, as shown in Fig. 9(c), it is possible to obtain a device capable of supporting a high current while still keeping a neatly marked NDR peak. We thus see that the desired characteristics of devices consisting only of one nonlinear component can be fine tuned by introducing nonlinearity in the other component, or improved by suitably combining both.

IV. CONCLUSIONS

In this concluding section of the paper, we summarize briefly what are our main findings on the transport properties of nonlinear DBS. A first overall conclusion is that the behavior of such kind of devices changes quite a bit when the nonlinearity of the system changes. This is very important: Keeping in mind that the nonlinear coefficients we have been handling include the contribution of the amplitude of the wavefunction, it is immediately understood that a device, built up from specific materials with specific and constant nonlinear characteristics, will change dramatically its response if the amplitude of the incoming wavefunction is also modified. This in turn can be related to the incoming current density. Clearly, a result like this paves the way to the search for devices with particular features arising from nonlinearity. We have to remind here that even if we have been discussing the outcome of our work in terms of electron transport, it can be straightforwardly translated to optical contexts, which gives further relevance to our results in view of the increasing importance of nonlinear optical phenomena for communications. In this respect, we want to stress that for that application the control of the nonlinearity of the devices by the incoming wave is even easier to realize.

Being more specific, we have found that devices with nonlinear barriers and negative, i.e., self-attractive nonlinearity, definitely show an increase of the current as compared to the linear case. This fact is not strange once it is realized that the role of nonlinearity in this case is to reduce the barriers. Roughly speaking, nonlinear barrier DBS begin transporting current for lower voltages; afterwards, they exhibit constant or slowly increasing characteristics for a range of voltages, which ends up in a

NDR region. The features of the $j - V$ curves are of course smoothed when the temperature is raised up to room values, a conclusion which applies to all the nonlinearities considered in this work. On the other hand, if the DBS is equipped with a nonlinear well, the device has more striking properties: In the lowest nonlinearity situation, it exhibits highly nonlinear properties, such as two NDR peaks; intermediate values of the nonlinear contribution will strongly suppress the current, and, finally, high nonlinearities lead to a quasi-linear current-voltage characteristic, with the RT peak being shifted to lower voltages and the current slightly increased. This is a peculiar property, and therefore we want to draw the readers' attention to the curious fact that nonlinear well DBS behave more differently from the linear case in the small nonlinearity situation. If we take also into account the suppression of the current for intermediate nonlinear values, it is evident that this kind of devices is the most appealing candidate for new applications. Finally, we have briefly pointed out some examples of combining both nonlinearities, and we have seen that it is possible to obtain clearer NDR peaks or higher conductivities (or both) by appropriately choosing the two components of the DBS to be nonlinear.

In view of this report, we feel we can conjecture that complex structures consisting of a number of nonlinear DBS will also exhibit very peculiar properties. One can think, for instance, of a system built up of nonlinear well DBS. If the input to such device is of high amplitude, the first DBS components will behave quasi-linearly, letting the current pass through them. The deviation from unity of the transmission coefficient will make decrease the amplitude, thus reaching the region for which the current is severely suppressed. This, in turn, would give rise to current in the remainder of the structure, because then it would behave more nonlinearly (as discussed above) allowing for transmission of the wavepacket. We would have thus designed a device which would transport current differently as a function of its length. Another possibly relevant remark relates to the mutual influence of disorder and nonlinearity, and applies to the case of nonlinear barrier DBS. It is clear that if a superlattice made of linear DBS is built, the imperfections introduced during the growth will lead to a mismatch among the resonant levels of neighboring wells and as consequence to a loss of quantum coherence leading to poor transport properties. Nonlinear barrier DBS will be much more robust against growth imperfections, as they have a plateau-like current behavior for a range of voltages, which makes irrelevant the exact matching of quasi-levels. The conclusion is once more that nonlinearity would help transport even in the presence of disorder. In any event, a detailed study of more complex structures is necessary to clarify and put on firm grounds all these ideas.

We finish by briefly pointing out another group of open questions which arise in view of our work. Further extensions of the present work to study nonlinear dynamical response of DBS on external ac bias would be

of great interest to shed light on related problems like bistability,¹⁶ noise characteristics,¹⁷ and RT at far infrared frequencies¹⁸ under the influence of inelastic scattering channels as those described here. Besides that, the above mentioned highly nonlinear limit could also be interesting, for nonlinearity is always susceptible to give rise to new and unexpected features. If these new features were seen in our model it would be a very exciting development. If materials with suitable characteristics were found, and that is to be expected, experiments could be made to check the predictions: If the model were wrong, that would establish its range of validity, whereas if the predictions were correct, this work could pave the way to a new family of devices and applications.

ACKNOWLEDGMENTS

We are very thankful to Paco Padilla for useful discussions. A. S. acknowledges partial support from C.I.C. y T. (Spain) through project No. PB92-0248 and by the European Union Human Capital and Mobility Programme through contract ERBCHRXCT930413.

APPENDIX: NONLINEARITY SIGN

In this appendix, we give mathematical reasons why α and β (or $\tilde{\alpha}$ or $\tilde{\beta}$) should be negative by using Eq. (6). We focus in the study of the problem with $\tilde{\beta} = 0$ for simplicity, but similar considerations apply to the general case. With this assumption, the equation has the form

$$-q_{zz}(z) + \frac{1}{q^3(z)} + f_1(z)q(z) + f_2(z)q^3(z) = 0, \quad (A1)$$

where $f_1(z)$ and $f_2(z)$ are well-behaved functions. Let us now consider the discrete version of this equation, with the second derivative discretized in the usual way; denoting $q_n = q(z = n\Delta z)$ and $f_{in} = f_i(n\Delta z)$, $i = 1, 2$, with Δz being the integration step, Eq. (A1) can be rewritten as

$$q_{n+1} = 2q_n - q_{n-1} + (\Delta z)^2 \left[\frac{1}{q_n^3} + f_{1n}q_n + f_{2n}q_n^3 \right]. \quad (A2)$$

Notice that in this expression the sign of f_{2n} is the same as the sign of α and $\tilde{\alpha}$. Let us now consider Eq. (A2) for large q_n ; this is general, because if q is small the term q_n^{-3} will make it grow quite quickly. In this limit, Eq. (A2) can be approximately replaced by

$$\Delta q_{n-1} = \Delta q_n + (\Delta z)^2 f_{2n}q_n^3, \quad (A3)$$

where $\Delta q_n = q_n - q_{n+1}$, and we have cast the equation in this fashion because it is to be integrated backwards. Recalling the initial conditions (7), if N is the total number

of grid points, we have $q_N = q_{N-1} = k_L^{-1/2} > 0$. Therefore, we see that $\Delta q_{N-1} = 0$, and

$$\Delta q_{N-2} = (\Delta z)^2 f_{2n} k_L^{-3/2}. \quad (\text{A4})$$

We thus see that if f_{2n} is positive (and hence α) the first increment is positive, and so are the subsequent ones, leading to an exponential divergence of q , whereas if f_{2n} and α are negative, the increment is negative, and q decreases until the q_n^{-3} starts being relevant again. In this last case, it is possible that q reaches an equilibrium due to the balance of the two cubic terms, which was not for $\alpha > 0$. This is in fact seen in the numerical integration of Eq. (6), where q rapidly diverges if α is positive, unless, of course, α is positive but very small and/or the barrier (the region for α to influence q) is very narrow. In this last situation, however, the effect of α becomes negligible.

Physically, this can be understood as follows. Seeing z as a time variable, Eq. (A1) can be regarded, loosely speaking, as an evolution equation for q , which is equivalent to the following interpretation: Electrons impinge on the barrier from outside, and begin to tunnel through it, their wavefunction being real and exponentially increasing or decreasing. If α is positive, then if there were any charge density in the BDS, this would become even more repulsive, and the wavefunction would diverge even faster (numerically one always sees the exponentially growing part, of course). This instability is not present in the opposite case, where a negative α helps the electron tunnel across the barrier. Note that this reasoning does not apply to the full partial differential equation, which is the one we should deal with for that case by starting from the complete Schrödinger equation.

¹ J. C. Flores, J. Phys. Condens. Matter **1**, 8471 (1989); D. Dunlap, H.-L. Wu, and P. Phillips, Phys. Rev. Lett. **65**, 88 (1990); A. Bovier, J. Phys. A **25**, 1021 (1992); P. K. Datta, D. Giri, and K. Kundu, Phys. Rev. B **47**, 10727 (1993); S. N. Evangelou and A. Z. Wang, Phys. Rev. B **47**, 13126 (1993); P. K. Datta, D. Giri, and K. Kundu, Phys. Rev. B **48**, 16347 (1993); M. Hilke, J. Phys. A **27**, 4773 (1994).
² A. Sánchez and F. Domínguez-Adame, J. Phys. A **27**, 3725 (1994); A. Sánchez, E. Maciá, and F. Domínguez-Adame, Phys. Rev. B **49**, 147 (1994); (E) Phys. Rev. B **49**, 15428 (1994).
³ A. Sánchez, F. Domínguez-Adame, G. P. Berman, and F. Izrailev, Phys. Rev. B **51** Rapid Comm., in press (1995). [BYR545]
⁴ A. Sánchez and L. Vázquez, Int. J. Mod. Phys. B **5**, 2825 (1991); S. A. Gredeskul and Yu. S. Kivshar, Phys. Rep. **216**, 1 (1992).
⁵ M. I. Molina and G. P. Tsironis, Phys. Rev. Lett. **73**, 464 (1994).
⁶ C. Presilla, G. Jona-Lasinio, and F. Capasso, Phys. Rev. B **43**, 5200 (1991); G. Jona-Lasinio, C. Presilla, and F. Capasso, Phys. Rev. Lett. **68**, 2269 (1992).
⁷ W. Deering, M. I. Molina and G. P. Tsironis, Appl. Phys. Lett. **62**, 2471 (1993).
⁸ T. C. L. G. Sollner, W. D. Goodhue, P. E. Tannenwald, C. D. Parker, and D. D. Peck, Appl. Phys. Lett. **43**, 588 (1984).
⁹ B. Ricco and M. Ya. Azbel, Phys. Rev. B **29**, 1970 (1984).
¹⁰ F. Domínguez-Adame, E. Diez, and A. Sánchez, Phys. Rev. B **51**, in press (1995). [BU5179]
¹¹ E. Diez, A. Sánchez, and F. Domínguez-Adame, Phys. Rev. B **50**, 14359 (1994); F. Domínguez-Adame, E. Diez, and A. Sánchez, *ibid* **50**, 17736 (1994). E. Diez, A. Sánchez, and F. Domínguez-Adame, preprint [cond-mat/9501096](http://arxiv.org/abs/cond-mat/9501096) (unpublished).
¹² E. Diez, F. Domínguez-Adame, and A. Sánchez, Phys. Lett. A **198**, 403 (1995).
¹³ J. Callaway, *Quantum Theory of the Solid State* (Academic Press, CA, 1991), p 711.
¹⁴ E. Diez, A. Sánchez, and F. Domínguez-Adame (unpublished).
¹⁵ R. Knapp, G. Papanicolaou, and B. White, J. Stat. Phys. **63**, 567 (1991).
¹⁶ P. Hawrylak and M. Grabowski, Phys. Rev. B **40**, 8013 (1989).
¹⁷ A. L. Levy Yeyati and F. Flores, Phys. Rev. B **47**, 10543 (1993).
¹⁸ V. A. Chitta, C. Kutter, R. E. M. de Bekker, J. C. Maan, S. J. Hawksworth, J. M. Chamberlain, M. Henini, and G. Hill, J. Phys. Condens. Matter **6**, 3945 (1994).
¹⁹ E. Diez, F. Domínguez-Adame, and A. Sánchez, J. Appl. Phys., in press (1995).